

Exploring Generalized Gait Recognition: Reducing Redundancy and Noise within Indoor and Outdoor Datasets

Qian Zhou^{1*}, Xianda Guo^{1*†}, Jilong Wang², Chuanfu Shen³, Zhongyuan Wang^{1‡},
Hua Zou¹, Qin Zou¹, Chao Liang¹, Chen Long^{4,5}, and Gang Wu⁶

¹ School of Computer Science, Wuhan University ² USTC ³ SIAS, UESTC

⁴ CASIA, ⁵ Waytous ⁶ College of Information Engineering, Tarim university

zhouqian@whu.edu.cn, {xianda_guo, wzy_hope}@163.com

Abstract

Generalized gait recognition, which aims to achieve robust performance across diverse domains, remains a challenging problem due to severe domain shifts in viewpoints, appearances, and environments. While mixed-dataset training is widely used to enhance generalization, it introduces new obstacles including inter-dataset optimization conflicts and redundant or noisy samples, both of which hinder effective representation learning. To address these challenges, we propose a unified framework that systematically improves cross-domain gait recognition. First, we design a disentangled triplet loss that isolates supervision signals across datasets, mitigating gradient conflicts during optimization. Second, we introduce a targeted dataset distillation strategy that filters out the least informative 20% of training samples based on feature redundancy and prediction uncertainty, enhancing data efficiency. Extensive experiments on CASIA-B, OU-MVLP, Gait3D, and GREW demonstrate that our method significantly improves cross-dataset recognition for both GaitBase and DeepGaitV2 backbones, without sacrificing source-domain accuracy. Code will be released at https://github.com/liler3/Generalized_Gait.

1. Introduction

Gait recognition has gained increasing attention due to its ability to identify individuals from a distance in a contactless manner [26]. Compared to traditional biometrics such as face, iris, and fingerprints, gait recognition is inherently robust to changes in lighting, occlusion, and background, making it highly valuable for surveillance and security applications [8, 25]. With the rapid advancement of deep learning, state-of-the-art gait recognition methods

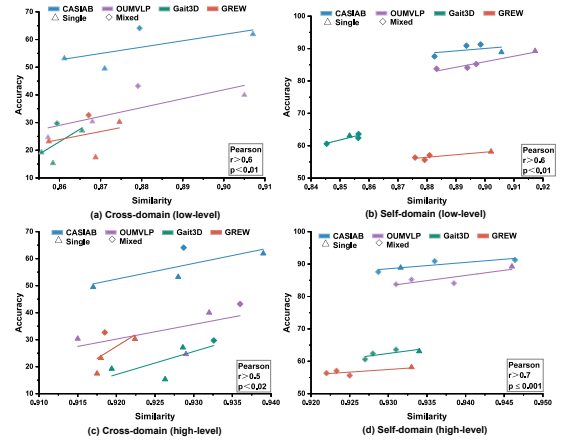


Figure 1. Relationship between dataset similarity and accuracy across different settings (low/high-level, cross/self-domain) of the GaitBase [6] model. Mixed training consistently improves performance, especially in cross-domain scenarios. Low-level and high-level indicate pixel-wise and feature-wise similarities, respectively.

have achieved impressive performance, surpassing 90% [6] accuracy on the OU-MVLP dataset [30] and 80% [21] on the GREW dataset [40], both of which contain thousands of subjects.

Despite these advancements, a critical challenge remains. Models trained on a single dataset often fail to generalize to unseen domains due to domain gaps, which arise from differences in viewpoints, environments, and subject appearances across datasets. These gaps cause data biases that lead to model biases, where models overfit to training-specific patterns instead of learning universal gait characteristics. Consequently, many existing methods [2, 4, 6, 17, 36] achieve high accuracy under in-domain settings but suffer severe performance degradation when evaluated across domains [33], limiting their applicability in unconstrained environments.

One widely adopted strategy to improve generalization

*These authors contributed to the work equally.

†Project leader; ‡Corresponding author.

is mixed-dataset training, where multiple datasets are aggregated to expose models to broader variations [23, 27]. While this approach improves robustness to some extent, simple aggregation introduces new obstacles, including inter-dataset optimization conflicts and redundant or noisy samples, both of which hinder effective feature learning.

To better understand these challenges, we investigate the relationship between dataset similarity and cross-domain recognition performance. Specifically, we measure low-level pixel-wise similarity using gait energy images (GEIs) and high-level feature-wise similarity using representations extracted from a pretrained CLIP [22] model. As shown in Figure 1, there exists a clear positive correlation between dataset similarity and cross-domain performance across both low-level and high-level feature spaces. Models trained on isolated datasets tend to perform poorly when tested on domains with low similarity, indicating limited generalization capability. In contrast, mixed-dataset training increases feature similarity and improves cross-domain accuracy, particularly when the domain gap is large.

However, mixed training alone does not fully resolve domain discrepancies. We observe that models trained on aggregated datasets still struggle on highly dissimilar domains, and sometimes degrade in self-domain performance. This indicates that while dataset diversity is beneficial, it also introduces optimization conflicts and exposes the model to redundant or noisy samples. In particular, controlled datasets such as CASIA-B [37] and OU-MVLP [30] provide clean and structured silhouettes but contain extensive redundancy, which can lead models to overfit to trivial patterns. In contrast, real-world datasets like Gait3D [39] and GREW [40] introduce diverse and realistic variations, but also suffer from significant noise due to occlusions, background clutter, and inconsistent viewpoints. Balancing these conflicting characteristics across datasets is critical for achieving scalable and robust gait recognition.

These findings motivate us to move beyond simple dataset aggregation by explicitly addressing optimization dynamics and data quality through targeted learning strategies. To this end, we propose a unified framework comprising two complementary components: a conflict-aware feature learning objective that decouples supervision across domains to prevent optimization interference, and a targeted dataset distillation strategy that prunes low-value samples based on redundancy and uncertainty. These components jointly improve training stability and cross-domain generalization, while preserving source-domain accuracy.

First, we introduce a separate triplet loss, where positive and negative pairs are sampled within the same dataset. By preventing the inclusion of cross-domain negatives, this formulation avoids forcing the network to separate samples from different domains in the embedding space, thus preserving domain-specific structure while promoting identity-

discriminative features. Second, we develop a targeted dataset distillation method to filter out the least informative 20% of samples based on two criteria: feature redundancy and prediction uncertainty. This strategy minimizes overfitting to trivial or noisy patterns, yielding a compact training set that supports better domain alignment and generalization. Additionally, we explore the role of Domain-Specific Batch Normalization (DSBN) [1] in the context of mixed-dataset gait recognition. While DSBN enhances performance within individual domains by preserving domain-specific statistics, our experiments reveal that it can adversely affect cross-domain generalization, highlighting the trade-off between specialization and transferability.

Our key contributions are summarized as follows:

- We propose a unified framework for generalized gait recognition that addresses two core challenges in mixed-dataset training: inter-dataset optimization conflicts and data redundancy.
- We design a separate triplet loss to decouple supervision signals across datasets, and a dataset distillation strategy that prunes 20% of low-value samples based on feature redundancy and prediction uncertainty.
- We conduct extensive experiments on four public gait datasets (CASIA-B [37], OU-MVLP [30], Gait3D [39], GREW [40]) and two backbone architectures (Gait-Base [6], DeepGaitV2 [5]), demonstrating that our method consistently improves cross-domain performance and generalizes effectively across model designs.

2. Related Works

2.1. In-Domain Gait Recognition

Most existing gait recognition methods are developed and evaluated in in-domain settings, where training and testing data are drawn from the same dataset. These approaches can be broadly grouped into appearance-based, model-based, and multi-modal methods. Appearance-based methods rely on silhouette sequences to model spatial-temporal gait dynamics. GaitSet [2] introduces a set-based representation without explicit temporal alignment. GaitPart [4] enhances discriminability by decomposing the body into local parts, while GaitGL [17] combines global and local feature branches. More recent efforts such as DeepGaitV2 [5], SPOSGait [13], and CLASH [3] explore 3D temporal modeling and NAS-based architecture optimization. Model-based methods utilize structured representations such as 2D/3D skeletons to extract motion cues. GaitGraph [31] models joint dependencies via graph convolutional networks, while SkeletonGait [7] uses heatmap encoding to enhance robustness against visual noise. In addition, several works like SkeletonGait++ [7] and MultiGait++ [16] explore multi-modal integration of silhouette, skeleton, and body-part features for improved performance under diverse

conditions. However, these works often overfit to dataset-specific characteristics such as viewpoint, background, and clothing, leading to significant generalization gaps in cross-domain scenarios.

2.2. Cross-Domain Gait Recognition

Cross-domain gait recognition aims to build models that generalize across datasets with diverse conditions, such as varying viewpoints, clothing, and backgrounds. A key challenge lies in mitigating domain shift without access to labeled target-domain data. Unsupervised domain adaptation (UDA) has been widely explored to align feature distributions between domains. GaitDAN [14] employs adversarial training to reduce cross-view discrepancies, while Ma *et al.* [20] propose a clustering-based pseudo-labeling strategy combined with a spatio-temporal aggregation network. GPGait [10] enhances pose-based adaptation via human-oriented transformation and part-aware graph convolutional learning. Trand [38] further improves UDA by discovering transferable local neighborhoods in the embedding space. Domain generalization approaches seek to improve robustness without using target-domain samples. CDTN [32] transfers latent representations through cross-domain mappings. BigGait [36] introduces a pipeline that leverages large vision models and a Gait Representation Extractor (GRE) to produce task-relevant features from generic embeddings, achieving strong performance in cross-domain evaluation. Jaiswal *et al.* [15] explore domain-specific adaptation modules designed for practical deployment under unknown conditions.

Despite these advances, most existing methods either depend on target-domain statistics or introduce auxiliary adaptation modules, while overlooking the challenges introduced by mixed-dataset training—such as inter-dataset optimization conflicts and data redundancy. These issues remain largely underexplored in current literature and motivate the need for more scalable, unified solutions.

2.3. Dataset Distillation

Dataset distillation aims to improve training efficiency by identifying and retaining only informative subsets of data. In image classification, early works have explored synthetic distillation [34], soft-label-based selection [28], and latent factorization for data compression [18]. More recent approaches improve distillation realism and diversity via patch recombination and retrieval-based strategies [29]. In the context of human analysis, data pruning and filtering techniques have been applied to face recognition [24], re-identification [35], and video understanding [11], where redundant or low-quality samples may impair generalization. However, in gait recognition, such strategies remain underexplored. Most existing methods either rely on full datasets or use naive sampling without explicitly analyzing

sample informativeness or cross-domain utility.

To date, no prior work systematically investigates sample-level selection under mixed-dataset training for gait. This gap limits the scalability of gait systems when facing large, heterogeneous training corpora.

3. Method

3.1. Learning from Multiple Gait Datasets

Gait recognition aims to identify individuals based on their walking patterns captured in visual sequences. Given a dataset \mathcal{D} consisting of N sequences and their identity labels, the goal is to learn an embedding function $f_\theta : X \rightarrow \mathbb{R}^m$ such that intra-class features are compact and inter-class features are well-separated.

In this work, we focus on a more practical and challenging setting where training data comes from multiple datasets. Let $\mathcal{D} = \{\mathcal{D}_1, \mathcal{D}_2, \dots, \mathcal{D}_n\}$ be a set of gait datasets collected under different environments, subjects, and camera views. This setting reflects real-world deployment conditions but also introduces significant domain discrepancies across datasets.

We adopt a leave-one-dataset-out evaluation protocol [12], where one dataset \mathcal{D}_d is held out as the test set, and the remaining datasets form the training set. This enables systematic evaluation of cross-dataset generalization.

The following sections describe our approach for improving recognition under this mixed-dataset setup, with a focus on addressing optimization conflict and training data redundancy.

3.2. Learning from Multiple Gait Datasets

Gait recognition aims to identify individuals based on their unique walking patterns extracted from visual data. Given a dataset \mathcal{D} consisting of N gait sequences and corresponding identity labels, the task is to learn a feature mapping function $f_\theta : X \rightarrow \mathbb{R}^m$, parameterized by θ , that embeds gait sequences into an m -dimensional feature space. This mapping ensures that sequences from the same individual are clustered closely while those from different individuals are pushed apart.

As illustrated in Figure 2, we extend this problem to a multi-dataset setting to improve model generalization across different domains. Specifically, we consider a collection of n datasets $\mathcal{D} = \{\mathcal{D}_1, \mathcal{D}_2, \dots, \mathcal{D}_n\}$, each acquired under different conditions and environments. To evaluate cross-domain generalization, we employ a leave-one-dataset-out [12] cross-validation strategy: in each iteration, one dataset \mathcal{D}_d is held out as the unseen test dataset $\mathcal{D}_{\text{test}} = \mathcal{D}_d$, while the remaining datasets are used for training, i.e., $\mathcal{D}_{\text{train}} = \mathcal{D} \setminus \{\mathcal{D}_d\}$.

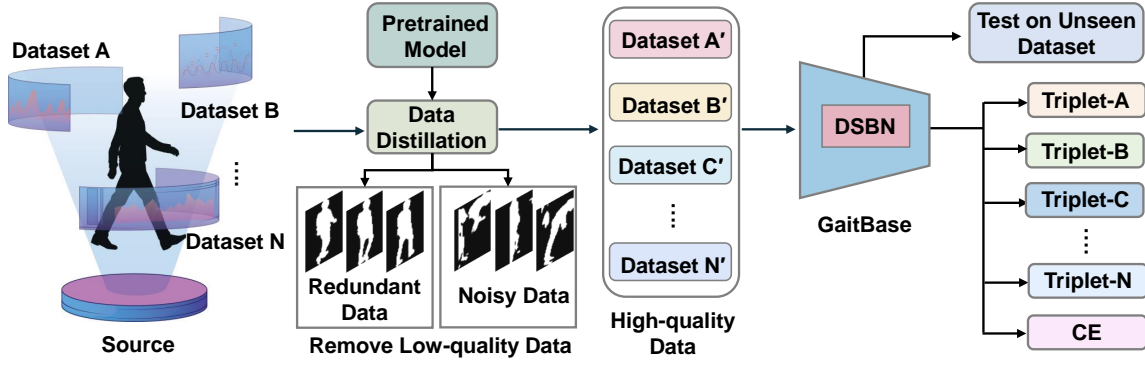


Figure 2. Overall framework of the proposed approach for cross-domain gait recognition. Each source dataset undergoes dataset distillation using a pre-trained model to filter out redundant and noisy samples, yielding high-quality subsets. These subsets are then combined to train the GaitBase [6] model with Domain-Specific Batch Normalization (DSBN) [1] and separate triplet losses, enhancing cross-dataset performance.

3.3. Dataset Distillation for Cross-Domain Robustness

While aggregating multiple datasets can improve generalization, it also introduces conflicts due to dataset-specific variations, such as redundant samples in controlled indoor datasets and noisy samples in outdoor datasets. To address this, we propose a dataset distillation strategy that selectively removes uninformative samples, allowing the model to learn more effectively from diverse datasets. This process is guided by pre-trained GaitBase [6] models trained on each full dataset. Distillation decisions are based on Euclidean distance computations and prediction consistency from these pre-trained models, ensuring reliable sample selection.

3.3.1. Reducing Redundancy in Indoor Datasets

In controlled environments, datasets often contain an excess of highly similar samples, contributing little additional diversity. These redundant samples may cause the model to overfit to trivial patterns, reducing its ability to generalize.

To mitigate this, we compute the mean Euclidean distance between each sample X_i and its negative samples (samples from different identities) in the feature space. A higher mean distance indicates that the sample is already well-separated from other identities and thus provides minimal contribution to the model’s discriminative learning. We define this measure as:

$$\text{mean_dist}(X_i) = \frac{1}{|N_i|} \sum_{X_j \in N_i} D(X_i, X_j), \quad (1)$$

where N_i represents the set of negative samples for X_i , and $D(X_i, X_j)$ denotes the Euclidean distance. Samples with the largest $\text{mean_dist}(X_i)$ values are considered redundant and are removed from the training set, reducing overfitting while improving generalization.

3.3.2. Removing Noisy Samples in Outdoor Datasets

Outdoor datasets introduce challenging conditions such as occlusions, background variations, and inconsistent silhouettes, which lead to noisy samples that can mislead the model. These samples often exhibit high intra-class variation and are more likely to be misclassified.

To identify and filter noisy samples, we compute the intra-class distance for each sample X_i , measuring its deviation from the centroid of its identity class μ_k :

$$\mu_k = \frac{1}{|\mathcal{C}_k|} \sum_{X_j \in \mathcal{C}_k} X_j, \quad (2)$$

$$\text{intra_dist}(X_i) = D(X_i, \mu_k), \quad (3)$$

where \mathcal{C}_k is the set of samples belonging to identity k . Samples with high intra-class distances are considered “hard samples” due to their deviation from the identity cluster, making them unreliable for training.

Additionally, we incorporate misclassification detection using predictions from the BNNeck [19] model. Samples are divided into p parts (due to the use of Horizontal Pyramid Pooling, HPP [9]), and misclassification is detected if any of the parts produces an incorrect prediction:

$$\text{failure}_i = \begin{cases} 1, & \text{if } \bigvee_{j=1}^p (\text{preds}_{i,j} \neq \text{labels}_i) \\ 0, & \text{otherwise} \end{cases} \quad (4)$$

We remove a proportion $n\%$ of samples that either have high intra-class distances or are frequently misclassified, ensuring that the retained samples are more reliable for cross-domain learning.

3.4. Separate Triplet Loss for Multi-Dataset Training

Triplet loss is commonly used in gait recognition to enforce compact intra-class clustering while maximizing inter-class

separation. However, when applied to multiple datasets, standard triplet loss can be problematic: negative samples from different datasets may exhibit distributional differences that distort the feature space.

To mitigate this issue, we compute triplet loss independently within each dataset, ensuring that each dataset maintains its unique characteristics without being influenced by negative samples from other datasets. The triplet loss for a given dataset \mathcal{D}_k is formulated as:

$$\text{Loss}_{\text{tri}}^k = [D(F_i, F_j) - D(F_i, F_k) + m]_+, \quad (5)$$

where F_i, F_j, F_k are the feature embeddings of the anchor, positive, and negative samples, respectively, $D(\cdot)$ represents the Euclidean distance, m is a margin enforcing separation, and $[\cdot]_+$ denotes the ReLU function to ensure non-negativity.

Our final objective combines the separate triplet losses for each dataset along with a cross-entropy loss for classification:

$$\text{Loss}_{\text{all}} = \sum_{k=1}^n w^k \text{Loss}_{\text{tri}}^k + \text{Loss}_{\text{ce}}, \quad (6)$$

where w^k is the triplet loss weight for the k -th dataset, and Loss_{ce} represents the cross-entropy loss.

By applying separate triplet loss, our approach effectively preserves dataset-specific structures while improving cross-domain generalization.

3.5. Domain-Specific Batch Normalization

Domain-Specific Batch Normalization (DSBN) is considered effective in unsupervised domain adaptation [1]. In this study, we extend it to mixed dataset training. Specifically, for each training dataset \mathcal{D}_k , we maintain independent BN layers with unique mean and variance parameters (μ_k, σ_k^2) , as well as scaling and shifting parameters (γ_k, β_k) . This setup allows the model to adapt to each dataset’s specific distribution without interference from others, ensuring domain-specific normalization.

During testing, for unseen datasets (*i.e.*, without corresponding BN layers), we use an averaged BN operation (BN_{avg}). Instead of averaging the statistics (mean and variance) directly, BN_{avg} applies each BN layer from the training datasets to the input and then averages the outputs:

$$\text{BN}_{\text{avg}}(x) = \frac{1}{n} \sum_{k=1}^n \text{BN}_k(x) \quad (7)$$

where n is the number of training datasets, and $\text{BN}_k(x)$ is the output from the BN layer of dataset \mathcal{D}_k . This approach provides an average normalization for unseen domains by leveraging the learned statistics from all training datasets.

4. Experiments

4.1. Datasets and Metrics

We evaluate our approach on four widely used gait datasets: CASIA-B [37], OU-MVLP [30], Gait3D [39], and GREW [40].

CASIA-B [37] is an indoor dataset with 124 subjects captured from 11 viewpoints (0° to 180° , at 18° intervals) under three conditions: normal walking (NM), walking with a bag (BG), and walking in a coat (CL). We follow the standard protocol [2], using 74 subjects for training and 50 for testing. NM#01-04 serve as the gallery, while NM#05-06, BG#01-02, and CL#01-02 form the probe set.

Dataset	Decay Steps (k)	Total Steps (k)
CASIA-B	(20, 40, 60)	80
OU-MVLP	(30, 60, 90)	120
Gait3D	(20, 40, 60)	80
GREW	(40, 80, 120)	160
CA, OU, G3D	(30, 60, 90)	120
CA, OU, GREW	(40, 80, 120)	160
CA, G3D, GREW	(40, 80, 120)	160
OU, G3D, GREW	(40, 80, 120)	160

Table 1. Training schedule across different datasets (steps in thousands).

OU-MVLP [30] is a large-scale dataset with 10,307 subjects captured from 14 viewpoints (0° to 90° and 180° to 270° , at 15° intervals). We use 5,153 subjects for training and the rest for testing, where Seq#01 is the gallery and Seq#00 is the probe.

Gait3D [39] is an unconstrained dataset collected in an indoor supermarket with 39 cameras, containing 4,000 subjects and over 25,000 sequences. The training set includes 3,000 subjects, while 1,000 subjects are used for testing. One sequence per subject serves as the probe, with the rest forming the gallery.

GREW [40] is a large-scale outdoor dataset with 26,345 subjects captured by 882 cameras in real-world environments. It comprises 128,671 sequences, split into a training set (20,000 subjects), validation set (345 subjects), and test set (6,000 subjects). Each test subject has four sequences, with two assigned as the gallery and two as the probe.

We use Rank-1 accuracy as the primary evaluation metric to compare recognition performance across datasets.

4.2. Implementation Details

All experiments are conducted using the PyTorch framework on $8 \times$ NVIDIA RTX 4090 GPUs, with GaitBase [6] or DeepGaitv2 [5] as the backbone. The input resolution is fixed at 64×44 pixels, and data augmentation techniques such as Random Perspective Transformation, Hor-

Table 2. Cross-dataset validation and mixed dataset training results for GaitBase [6] and DeepGaitV2 [5]. * denotes the distilled subset (20% data removal). Self-domain results are highlighted in light green, and cross-domain results in light yellow. Best and suboptimal results are marked in **bold** and underlined, respectively.

Training Set	GaitBase [6]				DeepGaitV2 [5]			
	CA	OU	G3D	GREW	CA	OU	G3D	GREW
CASIA-B	88.88	24.64	15.30	17.43	89.69	29.82	15.20	19.78
OU-MVLP	61.91	89.23	19.20	23.18	69.70	91.93	25.20	32.55
Gait3D	53.21	39.99	63.10	30.22	53.96	44.73	76.60	35.20
GREW	49.50	30.36	27.10	58.16	51.96	36.62	32.40	75.31
CA, OU, G3D	<u>90.90</u>	84.08	62.40	<u>32.68</u>	<u>91.45</u>	87.96	76.20	<u>36.70</u>
CA*, OU*, G3D*	89.70	83.83	62.10	32.90	90.89	87.55	75.80	37.00
CA, OU, GREW	91.28	85.22	<u>29.70</u>	57.05	91.98	88.12	<u>35.10</u>	74.68
CA*, OU*, GREW*	90.79	<u>85.32</u>	30.30	56.74	91.62	<u>87.80</u>	35.60	74.35
CA, G3D, GREW	87.60	<u>43.22</u>	<u>63.60</u>	56.34	88.55	<u>48.60</u>	<u>76.80</u>	74.15
CA*, G3D*, GREW*	87.49	44.58	64.00	<u>57.06</u>	88.40	49.30	77.20	<u>74.50</u>
OU, G3D, GREW	64.09	83.75	60.60	55.63	66.50	85.45	72.10	72.85
OU*, G3D*, GREW*	<u>63.72</u>	82.94	61.10	55.34	<u>65.93</u>	84.92	72.70	72.50
CA, OU, G3D, GREW	88.20	84.14	58.50	54.13	89.24	85.16	76.20	73.81
CA*, OU*, G3D*, GREW*	88.42	84.70	58.90	54.42	89.68	85.73	75.90	73.43

horizontal Flipping, and Random Rotation are applied. The model is trained with SGD, using an initial learning rate of 0.1, a weight decay of $5e^{-4}$, and a momentum of 0.9. The margin m in triplet loss is set to 0.2, following the GaitBase optimization strategy.

To enhance generalization, we adopt a mixed dataset sampling strategy, ensuring balanced representation from multiple datasets. For each dataset \mathcal{D}_i , P_i identities and K_i sequences per identity are randomly sampled, forming a mini-batch of size $B = \sum_{i=1}^n P_i \times K_i$. The dataset-specific batch sizes are: (16, 4) for CASIA-B [37], and (32, 4) for OU-MVLP [30], GREW [40], and Gait3D [39]. In mixed training, triplet loss weights w^k are set as: 0.2 for CASIA-B [37], 0.4 for OU-MVLP [30], 1.0 for GREW [40], and 0.8 for Gait3D [39]. Learning rate schedules follow a multi-step decay, detailed in Table 1.

4.3. Mixed Dataset Results

We present cross-dataset and mixed-dataset training results for both GaitBase [6] and DeepGaitV2 [5] in Table 2. Mixed-dataset training, which incorporates both in-the-lab and in-the-wild datasets, leads to moderate improvements in self-domain accuracy and substantial gains in cross-domain generalization for both models.

For example, integrating OU-MVLP [30], CASIA-B [37], and Gait3D [39] datasets achieves self-domain accuracies of 90.90% and 91.45% on CASIA-B [37] using GaitBase [6] and DeepGaitV2 [5], respectively. Similarly, combining CASIA-B [37], OU-MVLP [30], and GREW [40]

datasets yields the best self-domain accuracy of 91.98% on CASIA-B [37] using DeepGaitV2 [5], indicating that view-point diversity from OU-MVLP [30] enhances performance in controlled environments.

In cross-domain evaluations, mixed-dataset training notably outperforms single-dataset training. Specifically, training DeepGaitV2 [5] on CASIA-B [37], OU-MVLP [30], and GREW [40] datasets significantly improves accuracy to 35.10% on Gait3D [39], surpassing the single-dataset baseline by nearly 10%. Similarly, DeepGaitV2 achieves a remarkable cross-domain accuracy of 66.50% on CASIA-B [37] when trained jointly on OU-MVLP [30], Gait3D [39], and GREW [40], substantially outperforming individual dataset training.

4.4. Dataset Distillation Results

Figure 3 presents the results of the GaitBase [6] and DeepGaitV2 [5] models trained on different subsets obtained by removing varying proportions of low-quality samples. The impact of dataset distillation is evaluated in both self-domain and cross-domain settings, revealing how data quality influences model performance.

Indoor Datasets Results. For CASIA-B [37], removing up to 20% of redundant samples consistently improves both self-domain and cross-domain performance for GaitBase [6], with slight self-domain improvement (+0.08%) and noticeable cross-domain improvement on GREW [40] (+0.45%). DeepGaitV2 [5] exhibits a similar trend, achieving slightly lower self-domain improvement (+0.05%) and

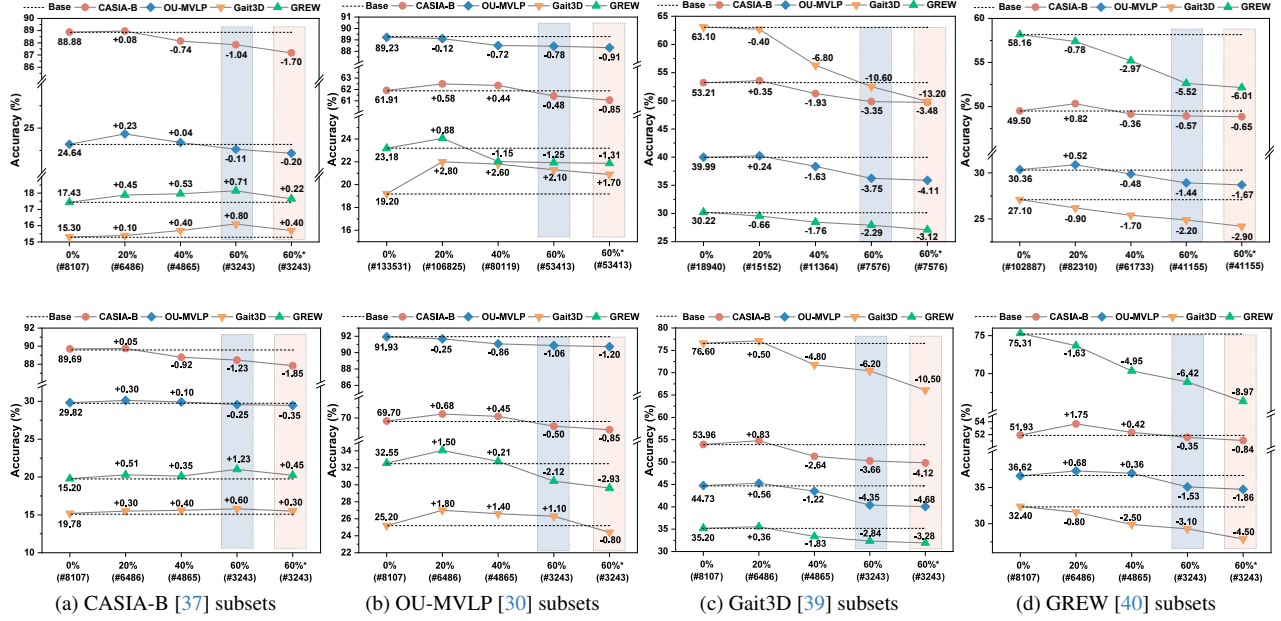


Figure 3. Cross-dataset validation results. The first row represents performance using GaitBase [6], while the second row represents performance using DeepGaitV2 [5]. The horizontal axis shows the proportion of low-quality data removed and the number of remaining gait sequences. "-" indicates performance drop, and "+" indicates improvement. "60%" means that 60% of samples are randomly dropped.

cross-domain accuracy on GREW [40] (+0.30%). As the removal ratio exceeds 20%, the self-domain accuracy slightly declines for both models; however, cross-domain accuracy continues improving, indicating that dataset distillation effectively reduces overfitting and enhances generalization. On OU-MVLP [30], a 20% data reduction preserves self-domain performance while substantially boosting cross-domain accuracy, with GaitBase [6] gaining +2.80% on Gait3D [39], and DeepGaitV2 [5] achieving a gain of +1.80%. Random sample removal also demonstrates modest cross-domain improvements, but targeted distillation consistently outperforms random removal across both models, highlighting its effectiveness in identifying redundant samples.

Outdoor Datasets Results. For Gait3D [39], removing 20% of noisy samples leads to minor changes in self-domain performance (-0.40% for GaitBase [6], +0.50% for DeepGaitV2 [5]) while simultaneously boosting cross-domain accuracy. DeepGaitV2 [5] notably achieves improvements of +0.83% on CASIA-B [37] and +0.56% on OU-MVLP [30], aligning with GaitBase’s trend but at higher performance levels. However, when removing over 40% of samples, self-domain accuracy for both models decreases significantly (e.g., GaitBase [6]: -6.80%, DeepGaitV2 [5]: -4.80%), indicating that outdoor datasets like Gait3D [39] critically depend on complex, diverse samples. The GREW [40] dataset displays a similar pattern, where removing 20% of noisy samples causes slight self-domain

performance drops but produces cross-domain gains. DeepGaitV2 [5] shows more robust cross-domain generalization, achieving a higher accuracy improvement (+1.75%) on CASIA-B [37] compared to GaitBase [6] (+0.82%). Random removal performs consistently worse, reinforcing that targeted noise removal significantly enhances cross-domain generalization.

Mixed Datasets Results. To further validate our dataset distillation approach, we train both GaitBase [6] and DeepGaitV2 [5] on distilled subsets from multiple datasets (20% removal ratio), as summarized in Table 2. Compared to full dataset training, distilled subsets yield comparable or improved self-domain accuracy, alongside consistent cross-domain gains. For example, training GaitBase [6] with distilled subsets of CASIA-B [37], Gait3D [39], and GREW [40] improves cross-domain accuracy on OU-MVLP [30] by +1.36% (from 43.22% to 44.58%) and self-domain accuracy on Gait3D [39] by +0.40% (from 63.60% to 64.00%). Similarly, DeepGaitV2 [5] trained on distilled subsets achieves even higher performance, with +0.70% cross-domain improvement on OU-MVLP [30] (from 48.60% to 49.30%) and a +0.40% self-domain accuracy increase on Gait3D [39] (76.80% to 77.20%). When training on CASIA-B [37], OU-MVLP [30], and GREW [40] datasets, distillation improves cross-domain accuracy on Gait3D [39] for both GaitBase [6] (29.70% to 30.30%) and DeepGaitV2 [5] (35.10% to 35.60%), further confirming the effectiveness and general applicability of our

Table 3. Ablation study on the effect of Domain-Specific Batch Normalization (BN) and Separate Triplet Loss (Tri) for GaitBase [6] and DeepGaitV2 [5]. Best and suboptimal results are marked in **bold** and underlined, respectively.

BN	Tri	CA [37]	OU [30]	G3D [39]	GREW [40]
GaitBase [6]					
\times	\times	<u>90.90</u>	84.08	62.40	<u>32.68</u>
\checkmark	\times	90.33	87.70	<u>63.60</u>	29.92
\checkmark	\checkmark	90.57	<u>87.55</u>	64.20	31.18
\times	\checkmark	92.20	85.83	63.00	33.56
DeepGaitV2 [5]					
\times	\times	91.45	87.96	76.20	36.70
\checkmark	\times	91.80	89.20	77.50	35.40
\checkmark	\checkmark	<u>93.12</u>	<u>89.05</u>	78.00	<u>35.90</u>
\times	\checkmark	93.63	88.35	<u>77.60</u>	37.20

distillation strategy.

These comprehensive experiments demonstrate that models trained on full datasets may overfit redundant or noisy samples, limiting their generalization. By selectively excluding low-quality samples, our dataset distillation strategy enables models to capture more generalizable gait representations, enhancing cross-domain robustness.

4.5. Ablation Study

To further analyze the impact of key components, we conduct ablation experiments on Domain-Specific Batch Normalization (DSBN) [1] and Separate Triplet Loss (Se_Tri), with results summarized in Table 3.

Effect of DSBN. Incorporating DSBN generally enhances self-domain performance but can adversely affect cross-domain generalization. For GaitBase [6], enabling DSBN significantly improves OU-MVLP [30] accuracy from 84.08% to 87.70% and moderately improves Gait3D [39] from 62.40% to 63.60%. For DeepGaitV2 [5], DSBN also notably enhances OU-MVLP [30] accuracy (from 87.96% to 89.20%) and Gait3D [39] (from 76.20% to 77.50%). However, cross-domain accuracy on GREW [40] notably decreases for both GaitBase [6] (32.68% to 29.92%) and DeepGaitV2 [5] (36.70% to 35.40%), indicating that DSBN’s alignment of dataset-specific statistics may limit feature transferability across diverse domains.

Effect of Separate Triplet Loss (Se_Tri). Employing Se_Tri consistently leads to performance gains in both self-domain and cross-domain settings. For GaitBase [6], applying Se_Tri significantly boosts CASIA-B [37] accuracy from 90.90% to 92.20%, with similar improvements in cross-domain accuracy on GREW [40] (32.68% to 33.56%). Similarly, DeepGaitV2 [5] achieves an increase in CASIA-B [37] accuracy from 91.45% to 93.63% and a notable gain in GREW [40] from 36.70% to 37.20%.

These improvements confirm that Se_Tri effectively mitigates cross-dataset optimization conflicts, encouraging the learning of discriminative, identity-specific gait features.

Combined Effect of DSBN and Se_Tri. When DSBN and Se_Tri are combined, the models exhibit mixed behaviors. For GaitBase [6], the combination improves self-domain accuracy slightly (*e.g.*, Gait3D [39] from 63.60% to 64.20%) but shows reduced cross-domain performance compared to using Se_Tri alone (GREW [40] accuracy drops from 33.56% to 31.18%). DeepGaitV2 [5] follows a similar trend; the combined setting achieves the highest Gait3D [39] accuracy (78.00%), indicating enhanced self-domain performance, but slightly reduces accuracy on GREW [40] compared to using Se_Tri alone (37.20% to 35.90%). This suggests DSBN may limit generalization improvements provided by Se_Tri.

5. Conclusion

This work addresses the challenge of cross-domain generalization in gait recognition by integrating mixed-dataset training with a targeted data distillation strategy. To mitigate the impact of data biases, we introduce separate triplet loss, ensuring dataset-specific feature learning while maintaining cross-domain compatibility. Additionally, we analyze Domain-Specific Batch Normalization (DSBN), which improves self-domain performance but negatively affects cross-domain generalization. To enhance robustness, our dataset distillation method removes redundant and noisy samples, refining training data and improving generalization. Experimental results show that training on distilled subsets (removing 20% of low-quality data) significantly enhances cross-dataset performance. With GaitBase [6], dataset distillation improves cross-domain accuracy by +1.4% on OU-MVLP [30] and +0.6% on Gait3D [39], while DeepGaitV2 [5] benefits even more, achieving greater improvements in challenging cross-domain settings.

References

- [1] Woong-Gi Chang, Tackgeun You, Seonguk Seo, Suha Kwak, and Bohyung Han. Domain-specific batch normalization for unsupervised domain adaptation. In *Proceedings of the IEEE/CVF conference on Computer Vision and Pattern Recognition*, pages 7354–7362, 2019. 2, 4, 5, 8
- [2] Hanqing Chao, Yiwei He, Junping Zhang, and Jianfeng Feng. Gaitset: Regarding gait as a set for cross-view gait recognition. In *Proceedings of the AAAI conference on artificial intelligence*, pages 8126–8133, 2019. 1, 2, 5
- [3] Huanzhang Dou, Pengyi Zhang, Yuhao Zhao, Lu Jin, and Xi Li. Clash: Complementary learning with neural architecture search for gait recognition. *IEEE Transactions on Image Processing*, 2024. 2
- [4] Chao Fan, Yunjie Peng, Chunshui Cao, Xu Liu, Saihui Hou, Jiannan Chi, Yongzhen Huang, Qing Li, and Zhiqiang He.

- Gaitpart: Temporal part-based model for gait recognition. In *Proceedings of the IEEE/CVF conference on computer vision and pattern recognition*, pages 14225–14233, 2020. 1, 2
- [5] Chao Fan, Saihui Hou, Yongzhen Huang, and Shiqi Yu. Exploring deep models for practical gait recognition. *arXiv preprint arXiv:2303.03301*, 2023. 2, 5, 6, 7, 8
- [6] Chao Fan, Junhao Liang, Chuanfu Shen, Saihui Hou, Yongzhen Huang, and Shiqi Yu. Opengait: Revisiting gait recognition towards better practicality. In *Proceedings of the IEEE/CVF conference on computer vision and pattern recognition*, pages 9707–9716, 2023. 1, 2, 4, 5, 6, 7, 8
- [7] Chao Fan, Jingzhe Ma, Dongyang Jin, Chuanfu Shen, and Shiqi Yu. Skeletongait: Gait recognition using skeleton maps. In *Proceedings of the AAAI Conference on Artificial Intelligence*, pages 1662–1669, 2024. 2
- [8] Claudio Filipi Gonçalves dos Santos, Diego de Souza Oliveira, Leandro A. Passos, Rafael Gonçalves Pires, Daniel Felipe Silva Santos, Lucas Pascotti Valem, Thierry P. Moreira, Marcos Cleison S. Santana, Mateus Roder, Jo Paulo Papa, et al. Gait recognition based on deep learning: a survey. *ACM Computing Surveys (CSUR)*, 55(2):1–34, 2022. 1
- [9] Yang Fu, Yunchao Wei, Yuqian Zhou, Honghui Shi, Gao Huang, Xinchao Wang, Zhiqiang Yao, and Thomas Huang. Horizontal pyramid matching for person re-identification. In *Proceedings of the AAAI conference on artificial intelligence*, pages 8295–8302, 2019. 4
- [10] Yang Fu, Shibe Meng, Saihui Hou, Xuecai Hu, and Yongzhen Huang. Gpgait: Generalized pose-based gait recognition. In *Proceedings of the IEEE/CVF International Conference on Computer Vision*, pages 19595–19604, 2023. 3
- [11] Shreyank N Gowda, Marcus Rohrbach, and Laura Sevilla-Lara. Smart frame selection for action recognition. In *Proceedings of the AAAI Conference on Artificial Intelligence*, pages 1451–1459, 2021. 3
- [12] Ishaan Gulrajani and David Lopez-Paz. In search of lost domain generalization. *arXiv preprint arXiv:2007.01434*, 2020. 3
- [13] Xianda Guo, Zheng Zhu, Tian Yang, Beibei Lin, Junjie Huang, Jiankang Deng, Guan Huang, Jie Zhou, and Jiwen Lu. Gait recognition in the wild: A large-scale benchmark and nas-based baseline. *arXiv e-prints*, pages arXiv–2205, 2022. 2
- [14] Tianhuan Huang, Xianye Ben, Chen Gong, Wenzheng Xu, Qiang Wu, and Hongchao Zhou. Gaitdan: Cross-view gait recognition via adversarial domain adaptation. *IEEE Transactions on Circuits and Systems for Video Technology*, 2024. 3
- [15] Nitish Jaiswal, Vi Duc Huan, Felix Limanta, Koichi Shinoda, and Masahiro Wakasa. Domain-specific adaptation for enhanced gait recognition in practical scenarios. In *Proceedings of the 2024 6th International Conference on Image, Video and Signal Processing*, pages 8–15, 2024. 3
- [16] Dongyang Jin, Chao Fan, Weihua Chen, and Shiqi Yu. Exploring more from multiple gait modalities for human identification. In *Proceedings of the AAAI Conference on Artificial Intelligence*, pages 4120–4128, 2025. 2
- [17] Beibei Lin, Shunli Zhang, and Xin Yu. Gait recognition via effective global-local feature representation and local temporal aggregation. In *Proceedings of the IEEE/CVF international conference on computer vision*, pages 14648–14656, 2021. 1, 2
- [18] Songhua Liu, Kai Wang, Xingyi Yang, Jingwen Ye, and Xinchao Wang. Dataset distillation via factorization. *Advances in neural information processing systems*, 35:1100–1113, 2022. 3
- [19] Hao Luo, Youzhi Gu, Xingyu Liao, Shenqi Lai, and Wei Jiang. Bag of tricks and a strong baseline for deep person re-identification. In *Proceedings of the IEEE/CVF conference on computer vision and pattern recognition workshops*, pages 0–0, 2019. 4
- [20] Kang Ma, Ying Fu, Dezhi Zheng, Yunjie Peng, Chunshui Cao, and Yongzhen Huang. Fine-grained unsupervised domain adaptation for gait recognition. In *Proceedings of the IEEE/CVF International Conference on Computer Vision*, pages 11313–11322, 2023. 3
- [21] Kang Ma, Ying Fu, Chunshui Cao, Saihui Hou, Yongzhen Huang, and Dezhi Zheng. Learning visual prompt for gait recognition. In *Proceedings of the IEEE/CVF Conference on Computer Vision and Pattern Recognition*, pages 593–603, 2024. 1
- [22] Alec Radford, Jong Wook Kim, Chris Hallacy, Aditya Ramesh, Gabriel Goh, Sandhini Agarwal, Girish Sastry, Amanda Askell, Pamela Mishkin, Jack Clark, et al. Learning transferable visual models from natural language supervision. In *International conference on machine learning*, pages 8748–8763. PmLR, 2021. 2
- [23] René Ranftl, Katrin Lasinger, David Hafner, Konrad Schindler, and Vladlen Koltun. Towards robust monocular depth estimation: Mixing datasets for zero-shot cross-dataset transfer. *IEEE transactions on pattern analysis and machine intelligence*, 44(3):1623–1637, 2020. 2
- [24] Torsten Schlett, Christian Rathgeb, Juan Tapia, and Christoph Busch. Double trouble? impact and detection of duplicates in face image datasets. *arXiv preprint arXiv:2401.14088*, 2024. 3
- [25] Alireza Sepas-Moghaddam and Ali Etemad. Deep gait recognition: A survey. *IEEE transactions on pattern analysis and machine intelligence*, 45(1):264–284, 2022. 1
- [26] Chuanfu Shen, Shiqi Yu, Jilong Wang, George Q Huang, and Liang Wang. A comprehensive survey on deep gait recognition: algorithms, datasets and challenges. *arXiv preprint arXiv:2206.13732*, 2022. 1
- [27] Cheng Shi, Yuchen Zhu, and Sibe Yang. Plain-det: A plain multi-dataset object detector. *arXiv preprint arXiv:2407.10083*, 2024. 2
- [28] Ilia Sucholutsky and Matthias Schonlau. Soft-label dataset distillation and text dataset distillation. In *2021 International Joint Conference on Neural Networks (IJCNN)*, pages 1–8. IEEE, 2021. 3
- [29] Peng Sun, Bei Shi, Daiwei Yu, and Tao Lin. On the diversity and realism of distilled dataset: An efficient dataset distillation paradigm. In *Proceedings of the IEEE/CVF Conference*

- on *Computer Vision and Pattern Recognition*, pages 9390–9399, 2024. [3](#)
- [30] Noriko Takemura, Yasushi Makihara, Daigo Muramatsu, Tomio Echigo, and Yasushi Yagi. Multi-view large population gait dataset and its performance evaluation for cross-view gait recognition. *IPSJ transactions on Computer Vision and Applications*, 10:1–14, 2018. [1](#), [2](#), [5](#), [6](#), [7](#), [8](#)
 - [31] Torben Teepe, Ali Khan, Johannes Gilg, Fabian Herzog, Stefan Hörmann, and Gerhard Rigoll. Gaitgraph: Graph convolutional network for skeleton-based gait recognition. In *2021 IEEE international conference on image processing (ICIP)*, pages 2314–2318. IEEE, 2021. [2](#)
 - [32] Suibing Tong, Yuzhuo Fu, and Hefei Ling. Gait recognition with cross-domain transfer networks. *Journal of Systems Architecture*, 93:40–47, 2019. [3](#)
 - [33] Jilong Wang, Saihui Hou, Xianda Guo, Yan Huang, Yongzhen Huang, Tianzhu Zhang, and Liang Wang. Gaitc3i: Robust cross-covariate gait recognition via causal intervention. *IEEE Transactions on Circuits and Systems for Video Technology*, 2025. [1](#)
 - [34] Tongzhou Wang, Jun-Yan Zhu, Antonio Torralba, and Alexei A Efros. Dataset distillation. *arXiv preprint arXiv:1811.10959*, 2018. [3](#)
 - [35] Yue Yao, Tom Gedeon, and Liang Zheng. Large-scale training data search for object re-identification. In *Proceedings of the IEEE/CVF Conference on Computer Vision and Pattern Recognition*, pages 15568–15578, 2023. [3](#)
 - [36] Dingqiang Ye, Chao Fan, Jingzhe Ma, Xiaoming Liu, and Shiqi Yu. Biggait: Learning gait representation you want by large vision models. In *Proceedings of the IEEE/CVF Conference on Computer Vision and Pattern Recognition*, pages 200–210, 2024. [1](#), [3](#)
 - [37] Shiqi Yu, Daoliang Tan, and Tieniu Tan. A framework for evaluating the effect of view angle, clothing and carrying condition on gait recognition. In *18th international conference on pattern recognition (ICPR’06)*, pages 441–444. IEEE, 2006. [2](#), [5](#), [6](#), [7](#), [8](#)
 - [38] Jinkai Zheng, Xinchun Liu, Chenggang Yan, Jiyong Zhang, Wu Liu, Xiaoping Zhang, and Tao Mei. Trand: Transferable neighborhood discovery for unsupervised cross-domain gait recognition. In *2021 IEEE International Symposium on Circuits and Systems (ISCAS)*, pages 1–5. IEEE, 2021. [3](#)
 - [39] Jinkai Zheng, Xinchun Liu, Wu Liu, Lingxiao He, Chenggang Yan, and Tao Mei. Gait recognition in the wild with dense 3d representations and a benchmark. In *Proceedings of the IEEE/CVF conference on computer vision and pattern recognition*, pages 20228–20237, 2022. [2](#), [5](#), [6](#), [7](#), [8](#)
 - [40] Zheng Zhu, Xianda Guo, Tian Yang, Junjie Huang, Jiankang Deng, Guan Huang, Dalong Du, Jiwen Lu, and Jie Zhou. Gait recognition in the wild: A benchmark. In *Proceedings of the IEEE/CVF international conference on computer vision*, pages 14789–14799, 2021. [1](#), [2](#), [5](#), [6](#), [7](#), [8](#)